CHIN. PHYS. LETT. Vol. 34, No. 9 (2017) 094101

# Effects of Breaking Waves on Composite Backscattering from Ship-Ocean Scene *

Jin-Xing Li(李金星), Min Zhang(张民)**, Peng-Bo Wei(魏鹏博)

*School of Physics and Optoelectronic Engineering, Xidian University, Xi'an 710071*

(Received 1 June 2017)

*The existence of the sea surface is bound to affect the electromagnetic (EM) scattering from marine targets. When dealing with the composite scattering from targets over a sea surface by applying high-frequency EM theories, the total scattering field can be decomposed into three parts in low sea states, namely, the direct scattering from the sea surface, the direct scattering from targets and the coupling scattering between the sea surface and targets. With regard to high sea states, breaking waves make the direct scattering from the sea surface and the coupling scattering more complicated. To solve this issue, a scattering model is proposed to analyze the composite scattering from a ship over a rough sea surface under high sea states. To consider the effect of breaking waves, a three dimensional geometric model is adopted together with Ufimtsev's theory of edge waves for the scattering from a breaker. In addition, the coupling scattering between targets and breaking waves is taken into account by considering all possible scattering paths. The simulated results indicate that the influence of breaking waves on the scattering field from the sea surface and on the coupling field is non-negligible, and the numerical results also show the effectiveness of the proposed scattering model.*

*PACS:* 41.20.Jb, 84.40.Xb, 91.50.Iv DOI: 10.1088/0256-307X/34/9/094101

Composite EM scattering from targets over a rough sea surface has been studied by many researchers[1−12] due to its great significance to target detection and recognition in the marine environment. In general, previous works have mostly focused on low sea states. However, it is an undeniable fact that a sea surface may be in a high sea state, and the existence of abnormal structures, such as breaking waves, is bound to affect the EM scattering from marine targets in this case. Due to this reason, this work focuses on the composite backscattering from a complex ship target over a rough sea surface under high sea states.

Based on the truth that both the sea surface and marine targets are electrically large, high-frequency asymptotic algorithms[10−12] are widely adopted to deal with the EM scattering problems from the composite ship-ocean scene for the reason of lower memory costs and higher computation efficiency. The high-frequency asymptotic algorithms usually decompose the total scattering field into three parts, namely, the direct scattering from the sea surface and from targets respectively, and the coupling scattering between them.

To generate the scattering field from sea surface $\boldsymbol{E}_{\rm sea}$, the EM model in our earlier work[13] is utilized, in which the waves on the sea surface are divided into non-breaking waves and breaking waves. The scattering from non-breaking waves is studied based on the capillary wave modification scattering facet model, while the scattering from breaking waves is investigated based on Ufimtsev's theory of edge waves[14] for diffraction from the wave crest. The advantage of this model is that the coverage of breaking waves on the sea surface depends on the wind speed, thus it is suitable for the scattering from sea surfaces under both low and high sea states.

For the scattering from a target with a complex geometric structure, the multiple reflections make significant contributions to the scattering field. To take this effect into consideration, the geometrical optics and physical optics (GO-PO) hybrid method[9,11] is employed to evaluate the scattering field from the target $\boldsymbol{E}_{\rm t}$ because of its intelligible mechanism and reasonable results.

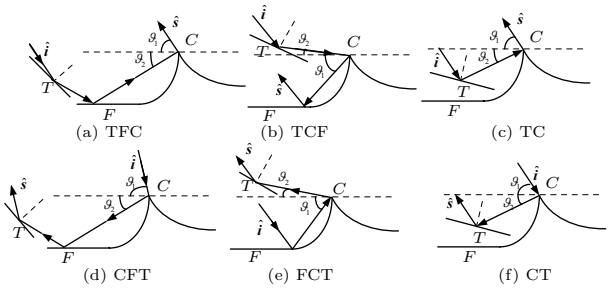


**Fig. 1.** The possible coupling scattering paths between a patch on target and a breaking wave.

In addition, the GO-PO hybrid method is utilized for the calculation of the coupling scattering field $\boldsymbol{E}_{\rm cou_nbw}$ between the ship target and non-breaking waves on the sea surface as well. The details are available in Ref. [11]. However, when it comes to the coupling field $\boldsymbol{E}_{\rm cou_bw}$ between the ship target and breaking waves, the GO-PO hybrid method loses its efficacy. To solve this problem, by referring to the idea of ray

*Supported by the National Natural Science Foundation of China under Grant No 61372004, the Fundamental Research Funds for the Central Universities, and the Foundation of Science and Technology on Electromagnetic Scattering Laboratory.

**Corresponding author. Email: mzhang@mail.xidian.edu.cn

© 2017 Chinese Physical Society and IOP Publishing Ltd

tracing in the GO-PO method, we analyze the possible coupling scattering paths between breaking waves and the target, as shown in Fig. 1.

The three paths in Figs. 1(a)–1(c) are the coupling scattering from the $m$th patch (indicated with T in Fig. 1) on target to the $p$th breaking wave. First, the incident wave is scattered from the target T to the sea surface near the foot F of a breaking wave and then scattered at the wave crest C and finally reflected to the radar, which is marked as the target-foot-crest (TFC) path. Secondly, the incident wave is firstly scattered on the target and then scattered at the wave crest, and the third at the sea surface near the foot of the breaking wave, namely, the target-crest-foot (TCF) path. Thirdly, the incident wave can be scattered from the target to the wave crest directly and then reflected to the radar, namely, the target-crest (TC) path. According to the three paths, the scattering field from a breaking wave is[13]

$$\begin{aligned}\boldsymbol{E}^{b,pm}_{\text{cou_bw}} = {} & \boldsymbol{E}_{1m}\frac{\sqrt{\Delta S}}{2\sqrt{\pi}}D_{\text{h,v}}(\vartheta_1,\vartheta_2)\\ & \cdot\frac{\exp(jkR)}{R}\sqrt{\frac{2\pi h a_{\text{c}}}{1-2jkh\sin\vartheta_2}}\\ & \cdot\exp\Big(-\frac{2ha_{\text{c}}k^2\cos^2\vartheta_2\sin^2\varsigma}{1-2jkh\sin\vartheta_2}\Big),\end{aligned}\tag{1}$$

where $\boldsymbol{E}_{1m}$ is the reflected field on the $m$th patch that can be calculated based on Fresnel's law, $\Delta S$ is the facet area on sea surface, $D_{\text{h,v}}$ is the total diffraction coefficient of the three paths under horizontal or vertical polarization, $k$ is the incident wave number, $h$ is the height of the breaking wave, $a_{\text{c}}$ is the radius of curvature of the wave crest, $\varsigma$ is the angle between the breaking wave propagation direction and the projection of the backscattered wave vector onto the sea surface, $\vartheta_1$ is related to the incident/scattering angle, and $\vartheta_2$ is related to the normal vector of the patch and the incident direction, which can be calculated based on the Fresnel equation. In Fig. 1, $\hat{\boldsymbol{i}}$ and $\hat{\boldsymbol{s}}$ are the unit vectors along the incident direction and the scattering direction, respectively. One thing should be pointed out is that the parameters of different breaking waves on sea surface are random within certain numerical ranges. The numerical ranges for different parameters are different and they can be found in detail in Ref. [13].

Similarly, there are also three paths contributing to the coupling scattering field from the $p$th breaking wave to the $m$th patch on target. First, the incident wave is scattered at the crest and the foot position, then scattered to the target, i.e., the crest-foot-target (CFT) path. Secondly, the incident wave is scattered at the foot position, then at the crest and scattered to the target, namely, the foot-crest-target (FCT) path. The third path is that the incident wave is scattered only at the crest and then scattered to the target, which is referred to as the crest-target (CT) path.

For these three paths, one can calculate the reflected field on a breaking wave based on Eq. (1) by replacing $\boldsymbol{E}_{1m}$ with the incident wave vector $\boldsymbol{E}_i$, and then the electric current $\boldsymbol{M}_{\text{mpi}}$ and the magnetic current $\boldsymbol{J}_{\text{mpi}}$ of the $m$th patch on the target, which are induced by the scattered wave from the $p$th breaking wave following the $i$th path ($i = 1$, 2 and 3 correspond to Figs. 1(d), 1(e) and 1(f), respectively), can be obtained. Then the scattering field can be calculated based on the physical optics (PO) formula, i.e.,

$$\begin{aligned}\boldsymbol{E}^{t,mp}_{\text{cou_bw}} = {} & \sum_{i=1}^{3} jk\frac{\exp(-jkR)}{4\pi R}\\ & \cdot\iint_S \hat{\boldsymbol{s}}\times(\boldsymbol{M}_{\text{mpi}}-\eta\hat{\boldsymbol{s}}\times\boldsymbol{J}_{\text{mpi}})\\ & \cdot\exp[jk(\hat{\boldsymbol{i}}_{\text{ri}}-\hat{\boldsymbol{s}})\cdot\boldsymbol{r}]dS,\end{aligned}\tag{2}$$

where $\eta$ is the impendence in free space, $\hat{\boldsymbol{i}}_{\text{ri}}$ is the unit vector of the reflected wave from the breaking wave following the $i$th path, and $\boldsymbol{r}$ is the position coordinate of the $m$th patch on the target. Finally, the coupling field between the ship target and breaking waves can be obtained by taking all of the six paths into consideration,

$$\boldsymbol{E}_{\text{cou_bw}} = \sum_{m=1}^{M}\sum_{p=1}^{N_1}(\boldsymbol{E}^{t,mp}_{\text{cou_bw}}\cdot\boldsymbol{\nu}_{\text{mp}} + \boldsymbol{E}^{b,pm}_{\text{cou_bw}}\cdot\boldsymbol{\nu}_{\text{pm}}),\tag{3}$$

where $N_1$ and $M$ are the total number of breaking waves and ship patches, respectively, $\boldsymbol{\nu}_{\text{mp}}$ is for the possible visibility of the scattered wave from the $p$th breaking wave to the $m$th patch on the target, while $\boldsymbol{\nu}_{\text{pm}}$ is the opposite. Both of them have two values, namely, zero and one, depending on whether the scattered wave is visible or not. Up to date, the coupling field between the target and sea surface is $\boldsymbol{E}_{\text{cou}} = \boldsymbol{E}_{\text{cou_nbw}} + \boldsymbol{E}_{\text{cou_bw}}$, and the total scattering field is easy to obtain by summing up the three parts of the contribution, that is,

$$\boldsymbol{E}_{\text{total}} = \boldsymbol{E}_{\text{cou}} + \boldsymbol{E}_{\text{t}} + \boldsymbol{E}_{\text{sea}}.\tag{4}$$

In the calculation, the amplitude of the incident wave can be set as 1 for convenience, then the total radar cross section (RCS) of the composite ship-ocean scene is

$$\sigma = \lim_{R\to\infty} 4\pi R^2\frac{|\boldsymbol{E}_{\text{total}}|^2}{|\boldsymbol{E}_i|^2} = \lim_{R\to\infty} 4\pi R^2|\boldsymbol{E}_{\text{total}}|^2.\tag{5}$$

To validate the complete scattering model by comparing the RCS results of a scene containing both breaking waves and targets with other universally accepted algorithms or measured data, we divide this problem into two parts. First, the effectiveness of scattering from the sea surface under a high sea state is

validated, as shown in Figs. 2(a) and 2(b) by comparing the normalized radar cross section (NRCS) over 100 samples with the SASS model[15] and with measured data in Ref. [16] for different incident angles. In the simulation, the wind speed $u_{10}$ is 13 m/s at 10 m height above the mean sea level, the frequency of incident wave is 14.6 GHz for Fig. 2(a), while it is 13.9 GHz for Fig. 2(b), the relative dielectric constant of sea water is calculated by the Klein and Swift model[17] at 20℃ and 3.5% salinity. Then for the effectiveness of the scattering model in a calm sea surface, the VV polarized RCS results from a perfect electric conductor (PEC) cubic with a side length of $2\lambda$ on a PEC square plane with a side length of $8\lambda$ are shown in Fig. 2(b), in comparison with those calculated by the multi-level fast multipole method (MLFMM) under monostatic configuration. Here $\lambda$ is the incident wavelength. The frequency of incident wave is 2 GHz and the incident angle varies from 0° to 90° in the $xoz$ plane. The comparison results show the availability of the breaking wave model and the feasibility of the scattering model proposed in this study.

Next, based on the proposed scattering model, backscattering RCS results of the ship model shown in Fig. 3 on a sea surface with a size of 90 m×90 m under different polarization modes are illustrated in Fig. 4. Meanwhile, the direct scattering fields from the sea surface and from the ship, the coupling field, and the total field are calculated in the cases with and without breaking waves. In the simulation, the frequency of the incident wave is 5 GHz. The wind speed $u_{10}$ is 10 m/s. The incident wave slants at $\theta_i = -80°$–$80°$ in the $xoz$ plane. For a negative incident angle, it means that the incident wave illuminates the composite scene along the positive $x$ direction, while a positive incident angle means the opposite.

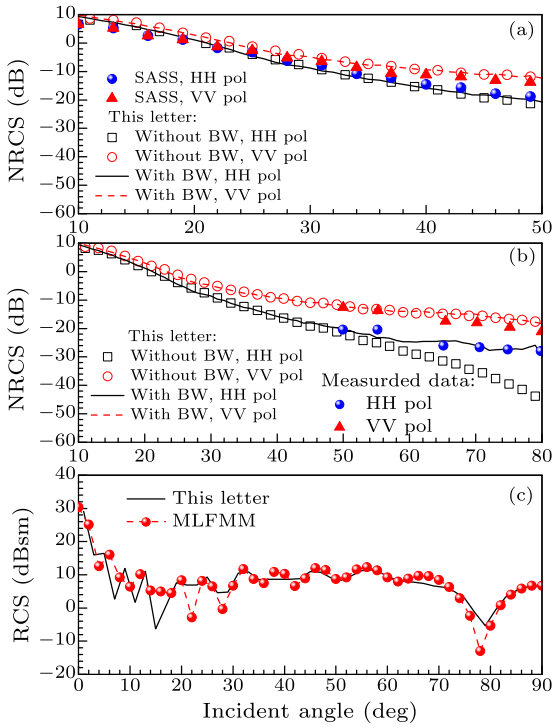


**Fig. 2.** Validation of the proposed model. (a) Comparison of NRCS results with the SASS model. (b) Comparison of NRCS results with measured data. (c) Comparison of RCS results with MLFMM. BW: breaking waves.

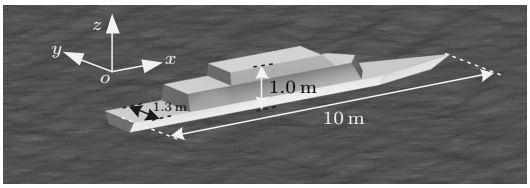


**Fig. 3.** Geometric dimensioning of the ship model.

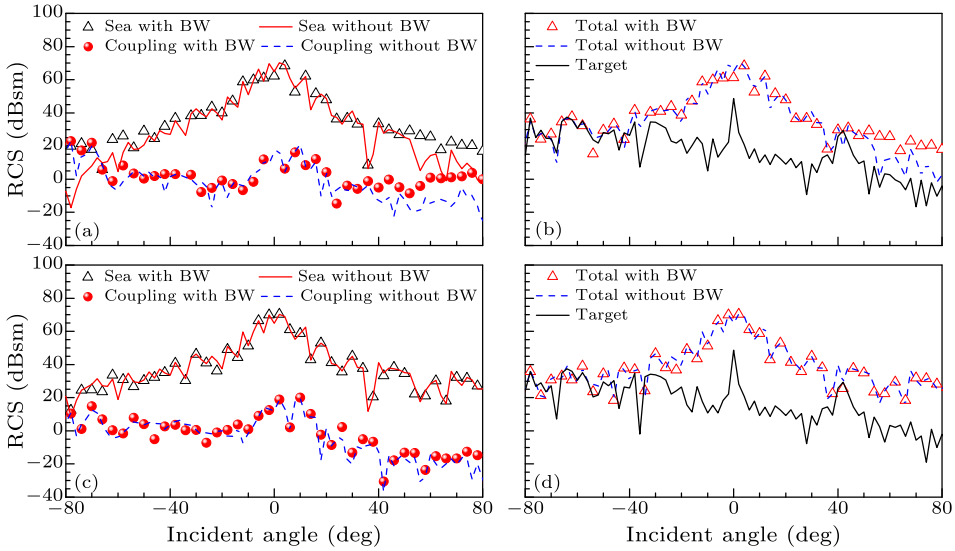


**Fig. 4.** Comparison of different components of the RCS of the ship model on a sea surface. The wind speed is 10 m/s. Here (a) and (b) are the results under HH polarization while (c) and (d) are the results under VV polarization.

From the HH polarized results shown in Figs. 4(a) and 4(b), one can see that the influence of breaking waves is mainly on the direct scattering field from the sea surface and on the coupling field, and they ultimately lead to an obvious effect on the total field especially for large incident angles. Furthermore, through comparing the coupling field under different incident angles, one can see the asymmetry caused by the ship model. When the wave illuminates the scene along the positive $x$ direction, the coupling field between non-breaking waves and the ship, which resulted from the dihedral corner structure at the ship stern, is so large that the coupling field between breaking waves and the ship is insignificant. This phenomenon can only indicate that the contribution of breaking waves is not very obvious compared with such a strong scattering source, but it does not mean that the contribution of breaking waves can be ignored. Furthermore, the contribution from breaking waves is obvious when the wave illuminates the scene along the negative $x$ direction because there are no structures approximately perpendicular to the sea surface at the ship bow.

On the other hand, by observing the VV polarized results in Figs. 4(c) and 4(d), it can be seen that the contribution of breaking waves to the direct scattering field from the sea surface and the coupling scattering field is not evident compared with the HH polarized case. Moreover, in the former experiments on sea surface scattering, the above phenomenon has also appeared. Accordingly, the consistency reveals the reasonability of the proposed model.

In summary, we mainly focus on the EM scattering from a composite ship-ocean scene under high sea states. To take the effect of breaking waves into consideration in high sea states, we apply the model in our former work to study the scattering from a sea surface with breaking waves. In addition, the way to evaluate the coupling scattering field between breaking waves and the ship target are described. On this basis, a complete scattering model, which is able to evaluate the scattering from a composite ship-ocean scene under high sea states, is established in combination with the GO-PO hybrid method. Using the proposed model, the RCS results from a ship over an electrically large rough sea surface under different polarizations are studied and analyzed. The numerical results demonstrate the validity of the proposed model.

## References


[1] Xie T, Perrie W, Zhao S Z, Fang H, Yu W J and He Y J 2016 *Chin. Phys.* B **25** 074102
[2] Xie T, Zhao S Z, Perrie W, Fang H, Yu W J and He Y J 2016 *Chin. Phys.* B **25** 064101
[3] Burkholder R J, Pino M R and Obelleiro F 2001 *IEEE Antennas Propag. Mag.* **43** 25
[4] Luo W, Zhang M, Zhou P and Yin H C 2009 *Chin. Phys. Lett.* **26** 114101
[5] Xu F and Jin Y Q 2009 *IEEE Trans. Antennas Propag.* **57** 1495
[6] Deng F S, He S Y, Chen H T, Hu W D, Yu W X and Zhu G Q 2010 *IEEE Trans. Antennas Propag.* **58** 1625
[7] Zhu Y J, Jiang Y S, Zhang C H and Xin C W 2014 *Acta Phys. Sin.* **63** 164202 (in Chinese)
[8] Yu W D, Hua F, Jin M B, Pan Z D and Yuan Y L 1998 *Chin. Phys. Lett.* **15** 931
[9] Wei P B, Zhang M, Niu W and Jiang W Q 2012 *IEEE Trans. Antennas Propag.* **60** 5278
[10] Li X F, Xie Y J, Fan J and Wang Y Y 2009 *Acta Phys. Sin.* **58** 908 (in Chinese)
[11] Zhang M, Zhao Y, Li J X and Wei P B 2017 *IEEE Trans. Antennas Propag.* **65** 775
[12] Zhang M, Li L W, Li L X and Wu Z S 2007 *Chin. Phys. Lett.* **24** 1563
[13] Li J X, Zhang M, Fan W N and Nie D 2017 *IEEE Trans. Geosci. Remote Sens.* **55** 2313
[14] Ufimtsev P Y 1962 *Method of Edge Waves in the Physical Theory of Diffraction* (Moscow: Soviet Radio)
[15] Wentz F J, Peteherych S and Thomas L A 1984 *J. Geophys. Res.* **89** 3689
[16] Plant W J 2003 *Waves Random Complex Media* **13** 339
[17] Klein L A and Swift C T 1977 *IEEE Trans. Antennas Propag.* **25** 104